

## Synthesis and Optical Properties of Novel Nickel Disulfide Dendritic Nanostructures

Rui Luo, Xia Sun,<sup>†</sup> Lifeng Yan,<sup>††</sup> and Wenming Chen\*

Structure Research Laboratory and Department of Polymer Science and Engineering,  
University of Science and Technology of China, Hefei 230026, P. R. China

<sup>†</sup>Department of Physics, University of Science and Technology of China, Hefei 230026, P. R. China

<sup>††</sup>Department of Chemical Physics, University of Science and Technology of China, Hefei 230026, P. R. China

(Received February 19, 2004; CL-040189)

Dendritic NiS<sub>2</sub> nanostructures are successfully synthesized for the first time via the reaction between NiCl<sub>2</sub>·6H<sub>2</sub>O and CS<sub>2</sub> in poly(MMA-co-EA) gel using  $\gamma$  irradiation.

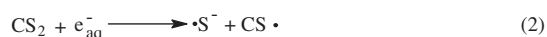
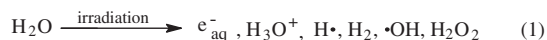
Transition metal dichalcogenides have drawn considerable attention owing to the large variety of their electrical, optical, and magnetic properties.<sup>1-3</sup> The synthesis of well-defined nanostructured semiconductor has recently been the focus of much attention because of the influence of their sizes and shapes on their electronic, optical and catalytic properties.<sup>4-6</sup> Dendritic nanostructures are one type of attractive supramolecular structures, and in the past few years, there are a variety of methods to be used for preparing dendritic nanostructures.<sup>7-9</sup> Dendritic fractals are generally observed in nonequilibrium growth phenomena; therefore, they can provide a natural framework for the study of disordered systems.<sup>10,11</sup> The diffusion-limited aggregation (DLA) model<sup>12,13</sup> and cluster-cluster aggregation (CCA) model<sup>11,14</sup> are widely used to explain and analyze these phenomena. However, to our knowledge, dendritic nanostructures of transition metal dichalcogenides have not been reported up to now.

In this article, we present a polymer-controlled growth method for fabricating NiS<sub>2</sub> dendritic nanostructures using  $\gamma$  irradiation at room temperature. The polymer used in this preparation process is poly(MMA-co-EA) gel (MMA: methyl methacrylate, EA: ethyl acrylate). In our synthetic process, first, the transparent solid poly(MMA-EA) gel was formed by irradiating a mixture consisting of 9-mL methyl methacrylate monomer and 4-mL ethyl acrylate monomer in the field of  $2.59 \times 10^{15}$  Bq <sup>60</sup>Co  $\gamma$ -ray source with rate of 67 Gy/min for 5 h. Second, poly(MMA-co-EA) gel was divided into pieces and then immersed in 50 mL of 0.2 mol/L CS<sub>2</sub> benzene solution. After changing the first immersion time from 5 to 10 h, gel **1** (5 h), **2** (8 h), **3** (10 h) were obtained. Third, these gels were taken out and washed with distilled water and acetone, then put into three portions of 50 mL of 0.1 mol/L NiCl<sub>2</sub>·6H<sub>2</sub>O aqueous solutions. When reaching the swelling equilibrium, 10-mL isopropanol was added. Next the three mixing systems were also  $\gamma$  irradiated with rate of 67 Gy/min for 24 h. The resulting brown solid product **1** (5 h), **2** (8 h), **3** (10 h) were filtered off, washed with distilled water and acetone several times, and finally heated in vacuum at 150 °C for 5 h. The possible formation mechanism of NiS<sub>2</sub> crystals could be explained as Scheme 1.<sup>15</sup>

X-ray powder diffraction (XRD) pattern of a sample shows the presence of diffraction peaks corresponding to the (200), (210), (211), (220), (311), and (230) planes of vaesite NiS<sub>2</sub> (JCPDS Card File, 11-0099).

From the field-emission scanning electron microscopy (FESEM) image of product **1**, we can observe that NiS<sub>2</sub> particles

were aggregating into the clusters and the whole clusters had not formed owing to the shortage of reactant CS<sub>2</sub>. The first immersion time of 5 h is insufficient for the gels to absorb enough CS<sub>2</sub>. FESEM images of products **2** and **3** indicate that the whole clusters had formed, and the clusters in product **3** are more compact and larger than those in product **2** (Figures 1a, b).



Scheme 1. Formation mechanism of NiS<sub>2</sub>.

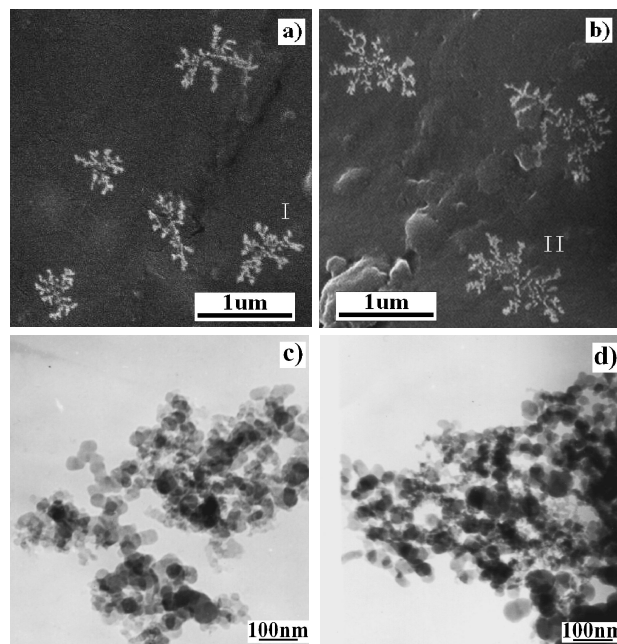
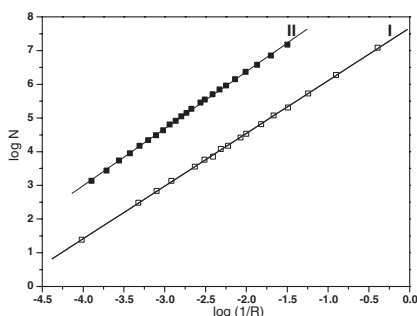


Figure 1. Field-emission scanning electron microscopy images of dendritic NiS<sub>2</sub> nanostructures, a) product **2**, b) product **3**. Transmission electron microscopy images of the products after being sliced into ultrathin film, c) product **2**, d) product **3**.

The reason for this result is that with the first immersion time changed from 8 h to 10 h, the swelling process in solutions led to increase the size of the polymer networks and the amount of the CS<sub>2</sub> in the networks for having not reached the swelling equilibrium. As shown in the transmission electron microscopy

(TEM) images, NiS<sub>2</sub> clusters in products **2** and **3** were composed of the spherical nanoparticles with narrow size distribution (Figures 1c, d). And the average particle sizes are both about 40 nm.

For measuring the dimensions of NiS<sub>2</sub> fractals, FESEM images were digitized, and the fractal dimension (D) was calculated by a box-counting method.<sup>16</sup> The digitized images were covered with boxes with a size R ( $R \leq 1$ ). The number of nonvacant boxes (N) could be counted. Images can be viewed as fractal ones if the plot of log N versus log(1/R) yields a straight line, namely  $N \sim R^{-D}$ . The slope of this line is the fractal dimension.



**Figure 2.** log N vs log(1/R) for the clusters (marked I, II) in Figures 1a, b (line I for cluster I in Figure 1a, line II for cluster II in Figure 1b).

Figure 2 shows the double logarithmic plot of N versus 1/R based on the cluster (marked I, II) in Figures 1a, b. The data points are well fitted by a straight line and the values of D are 1.56 (cluster I) and 1.69 (cluster II) respectively. The fractal dimension of any cluster is  $1.55 \pm 0.02$  in Figure 1a and  $1.69 \pm 0.01$  in Figure 1b. The aggregation patterns of NiS<sub>2</sub> nanoparticles in products **2** and **3** share common characteristics with DLA model such as the ramified structure starting from a unique seed. And the fractal dimension from Figure 1b is close to the one in DLA model ( $\approx 1.67$ ), while that from Figure 1a is smaller. It indicates that with the first immersion time gone, NiS<sub>2</sub> fractal patterns are more approximate to the DLA model. The fractal growth in the present case is believed to arise from the nucleation and growth of NiS<sub>2</sub> nanoparticles within a polymer matrix saturated with NiS<sub>2</sub> atoms produced by the reaction between NiCl<sub>2</sub>·6H<sub>2</sub>O and CS<sub>2</sub> by the radiation reduction process. The clusters are generated by the random walk movement of the NiS<sub>2</sub> atoms on to a growing cluster.

To investigate the intrinsic optical properties of the dendritic NiS<sub>2</sub> crystals, optical characterizations were carried out by UV-vis absorption and photoluminescence spectra. In Figure 3a, A sharp absorption peak at 283.5 nm ( $E_g = 4.38$  eV) (curve 2) is found for products **2** and **3** dispersed in benzene, with poly(MMA-co-EA) gel dispersed in benzene as reference. While for product **1**, no absorption peak is observed (curve 1). Figure 3b shows the photoluminescence (PL) spectrum of NiS<sub>2</sub> crystals. In this figure, the excitation wavelength was 266 nm and the filter wavelength was 310 nm. Two emission peaks at 336 and 355 nm are found for products **2** and **3**. The highly structured shape of the emission suggests that the interaction is not of an excimer,<sup>17</sup> but rather a consequence of intermolecular exciton interactions.<sup>18</sup> While for product **1**, there is no emission peak. On the basis of above results, it can be found that the optical properties of NiS<sub>2</sub> crystals are strongly depended on its structure.

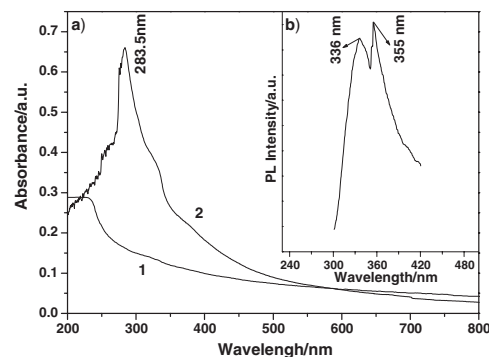


**Figure 3.** a) UV-vis absorption spectra of NiS<sub>2</sub> crystals (curve 1 for product **1**, curve 2 for product **2**, **3**). b) Photoluminescence spectra of NiS<sub>2</sub> crystals in product **2**, **3** (excitation wavelength was 266 nm).

A literature search shows that investigation on similar optical properties of NiS<sub>2</sub> has not been reported so far.

In this synthesis route, when poly(MMA-co-EA) gel was immersed in the benzene solution containing CS<sub>2</sub> less than 5 h, only NiS<sub>2</sub> nanospheres were obtained. While the time was prolonged to more than 12 h until poly(MMA-co-EA) gel became very soft, no dendritic crystals were formed because the gel networks was destroyed. The mechanism is the different length of the first immersion time altered the polymer networks of the absorbent correspondingly, and then the polymer networks affect the aggregation of NiS<sub>2</sub> particles. In conclusion, dendritic NiS<sub>2</sub> nanostructures have been prepared using poly(MMA-co-EA) gel as a host. We think this work could be of interest in that it provides the first example of transition metal dichalcogenides of dendritic nanostructures as well as suggests a new way to prepare similar structures of hybrid materials.

#### References

- 1 H. S. Jarrett, W. H. Cloud, R. J. Bouchard, S. R. Butter, C. G. Frederick, and J. L. Gilson, *Phys. Rev. Lett.*, **21**, 217 (1968).
- 2 J. M. Honig and Spelik, *J. Chem. Mater.*, **10**, 2910 (1998).
- 3 A. Ennaoui, S. Fiechter, W. Jaegermann, and H. Tributsch, *J. Electrochem. Soc.*, **133**, 97 (1986).
- 4 S. H. Yu and M. Yoshimura, *Adv. Mater.*, **14**, 296 (2002).
- 5 X. G. Peng, L. Manna, W. D. Yang, J. Wickham, E. Scher, A. Kadavanich, and A. P. Alivisatos, *Nature*, **404**, 59 (2000).
- 6 L. Manna, E. C. Scher, and A. P. Alivisatos, *J. Am. Chem. Soc.*, **122**, 12700 (2000).
- 7 S. T. Selvan, *Chem. Commun.*, **1998**, 351.
- 8 J. P. Xiao, Y. Xie, R. Tang, M. Chen, and X. B. Tian, *Adv. Mater.*, **13**, 1887 (2001).
- 9 Y. Zhou, S. H. Yu, C. Y. Wang, X. G. Li, Y. R. Zhu, and Z. Y. Chen, *Adv. Mater.*, **11**, 850 (1999).
- 10 T. A. Witten and L. M. Sander, *Phys. Rev. Lett.*, **47**, 351 (1981).
- 11 P. Meakin, *Phys. Rev. Lett.*, **51**, 1119 (1983).
- 12 T. A. Witten and L. M. Sander, *Phys. Rev. Lett.*, **47**, 1400 (1981).
- 13 T. A. Witten and L. M. Sander, *Phys. Rev. B*, **27**, 5658 (1983).
- 14 M. Kolb, R. Botet, and R. Jullien, *Phys. Rev. Lett.*, **51**, 1123 (1983).
- 15 R. Janes, A. D. Stevens, and M. C. R. Symons, *J. Chem. Soc., Faraday Trans.*, **85**, 3973 (1989).
- 16 D. A. Russell, J. D. Hanson, and E. Ott, *Phys. Rev. Lett.*, **45**, 1175 (1980).
- 17 B. Broklehurst, D. C. Bull, M. Evans, P. M. Scott, and G. Stanney, *J. Am. Chem. Soc.*, **97**, 2977 (1975).
- 18 R. M. Hochstrasser and M. Kasha, *Photochem. Photobiol.*, **3**, 317 (1964).